molecular pharmaceutics

ARTICLE

pubs.acs.org/molecularpharmaceutics

Combination Anti-HIV Therapy with the Self-Assemblies of an Asymmetric Bolaamphiphilic Zidovudine/Didanosine Prodrug

Yiguang Jin,*[,†,‡] Rui Xin,[†,‡] Li Tong,[§] Lina Du,[†] and Miao Li[†]

[†]Department of Pharmaceutical Sciences, Beijing Institute of Radiation Medicine, Beijing 100850, China

[‡]Institute of Pharmacy, Pharmaceutical College of Henan University, Henan 475004, China

[§]College of Life Sciences, Beijing Normal University, Beijing 100875, China

Supporting Information

ABSTRACT: Combination anti-HIV therapy is important for AIDS treatment. A bolaamphiphilic prodrug, zidovudine-phosphoryl-deoxycholyl didanosine (ZPDD), was synthesized, combining zidovudine (AZT) and didanosine (ddI) in one molecule. As one lipid derivative of nucleosides, ZPDD showed special solubility with free soluble in chloroform and tetrahydrofuran but was slightly soluble in cyclohexane. The amphiphilicity of ZPDD was shown according to the monolayers at the air−water interface. ZPDD self-assembled to the spherical vesicles in water with 174 nm in size and −31.3 mV of zeta potential. The stability of assemblies depended on pH because the phosphoryl zidovudine group could release hydrogen ions. ZPDD was rapidly degraded to AZT in the plasma and tissues of mice. ZPDD self-assemblies had high anti-HIV activity in vitro with the half effective concentration (EC_{50}) of 5 nM. ZPDD self-assemblies may be targeting macrophages since ZPDD was found in macrophage-rich tissues in vivo and rapidly released AZT in the targeted tissues after intravenous administration to mice. The bioavailability of ZPDD was 90.5% and 30.8% for the intraperitoneal and oral administrations compared with the venous route. The self-assemblies of bolaamphiphilic prodrugs could simultaneously deliver two types of drugs to targeted tissues and would become a promising nanomedicine.

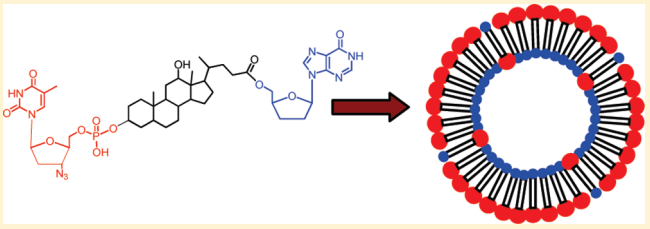

KEYWORDS: anti-HIV, bolaamphiphile, didanosine, prodrug, self-assembly, zidovudine

INTRODUCTION

Combination pharmacotherapy is commonly applied to treat AIDS, cardiovascular diseases, cancer, and so on.[1−4] Usually, it is difficult to simultaneously deliver all of the components of combination drugs to targeted cells and maintain an appropriate concentration. Two or more drugs are covalently combined to form codrugs to address the above problem though the conjugation may be complicated.[5−7] Carriers, such as liposomes and nanoparticles, could entrap two types of drugs, although the drug loading efficiency and the entrapment efficiency are generally low.[8,9] Furthermore, the carriers could be destroyed in circulation followed by rapid release of the cargos before reaching targets. It is necessary to develop a method to simultaneously deliver combination drugs to targets and release them.

Highly active antiretroviral therapy (HAART), combining at least three antiretroviral drugs, is a standard method to treat AIDS. Anti-HIV codrugs are also studied.[10] Dinucleoside compounds combine two nucleoside analogues with either one type or two types against viruses.[11,12] 3′-Azido-3′-deoxythymidilyl-(5′,5′)-2′,3′-dideoxy-5′-inosinic acid (AZT-P-ddI, IVX-E-59, Scriptene) was prepared and showed enhanced anti-HIV activity and selectivity in vitro compared with AZT and ddl alone. However, the pharmacokinetic study in humans showed that AZT-P-ddI was rapidly metabolized to β-glucuronide derivative of zidovudine (AZT) and a metabolite of didanosine (ddI) after intravenous (iv) infusion and oral administration.[13] Low bioavailability and weak targeting could lead to frequent high-dose administration of the drugs and further patient incompliance and drug resistance.[2] Macrophage is demonstrated as a reservoir of HIV. But many anti-HIV agents distribute little in the cells.[14,15] Nanoscale particles are preferred as the macrophage-targeted system based on optimization in circulation and macrophage-specific reorganization, so that the anti-HIV agent-loaded nanoparticulate systems are used for macrophage targeting.[16−18]

Bolaamphiphilic molecules or bolaamphiphiles are one special type of amphiphilic molecules and defined as the molecules containing a hydrophobic skeleton and two water-soluble groups on both ends.[19] The unique structure of bolaamphiphiles makes them to own some special functions different from traditional amphiphiles with one polar head. Bolaamphiphiles are inclined to form monolayers but not bilayers unless the hydrophobic skeleton is very soft and long, and the monolayer may be very strong even under harsh environments. Archaebacteria, one type of ancient bacteria with bolaamphiphilic monolayer membranes, can survive in the volcanic environment, enduring 80 °C high

Received: December 26, 2010
Accepted: May 9, 2011
Revised: April 27, 2011
Published: May 09, 2011

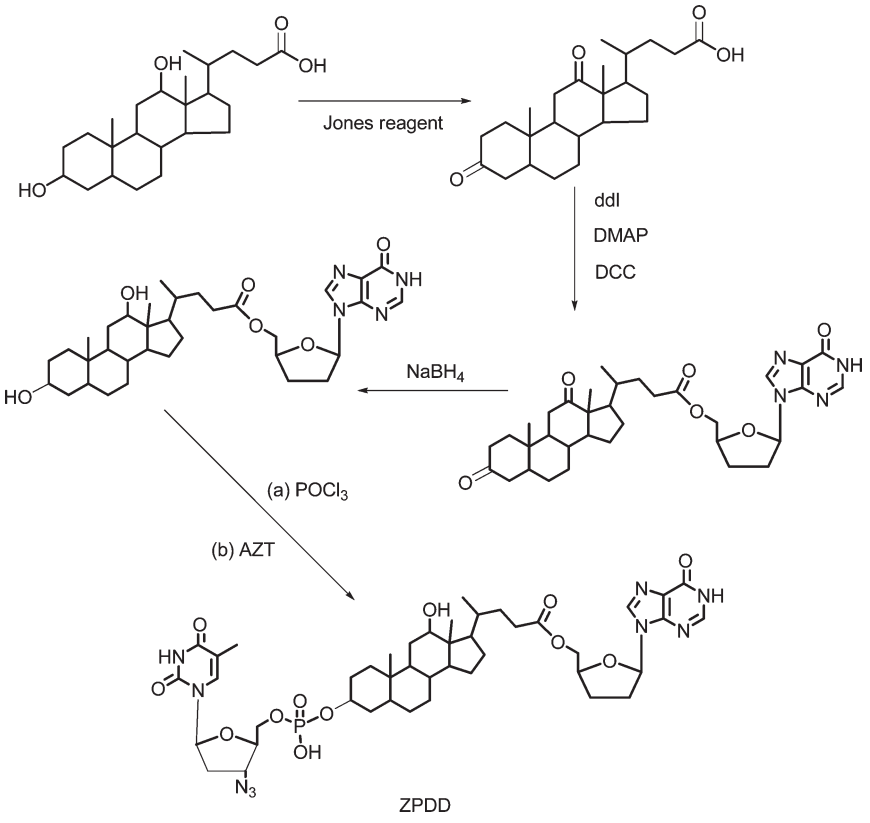

Figure 1. Synthesis route of ZPDD.

temperature and hot sulfuric acid.[20] Synthetic bolaamphiphiles may become the components of interesting structures, for example, nanowells, ion pores, electron conductors, DNA-like nanofibers, archaebacteria-mimic membranes, or nanotubes.[19,21−24] Some bolaamphiphiles are also used to form carriers to deliver genes or drugs.[25−27]

A method was developed to perform combination anti-HIV therapy with dual drugs in this study. A bolaamphiphilic prodrug, zidovudine-phosphoryl-deoxycholyl didanosine (ZPDD), was prepared. Zidovudine (AZT) and didanosine (ddI) were combined to treat AIDS.[28,29] ZPDD is the conjugate of the two drugs with deoxycholyl as the spacer. The prodrug can form the nanoscale self-assemblies with high anti-HIV activity in vitro and macrophage targeting in vivo. The assemblies could release parent drugs or active intermediates in the targeted tissues. ZPDD self-assemblies belong to the self-assembled drug delivery system (SADDS). SADDS has been developed in our lab for several years, defined as the self-assembled nanoparticulates of amphiphilic prodrugs. Many amphiphilic prodrugs were prepared and self-assembled to the assemblies with various morphologies though most of them only had one polar head and a long lipid chain.[30−33] Compared with traditional drug delivery systems, the unique advantages of SADDS include high stability, high drug loads, and controlled release in targets.[32]

EXPERIMENTAL SECTION

Materials. AZT and ddI were from Zhang Jiang Desano Science and Technology Co., Ltd., Shanghai, China. Deoxycholic acid was from Anhui Kebao Bioengineering Co., Ltd. (Anhui, China). Organic solvents were of analytical grade. Other chemicals were of reagent grade. Purified water was prepared with the Heal Force Super NW Water System (Shanghai Canrex Analytic Instrument Co. Ltd., Shanghai, China), and always used otherwise specially indicated. UV spectra and ^{1}H NMR (400 MHz) and ^{13}C NMR (100 MHz) spectra were recorded respectively on a Shimadzu UV-2501PC spectrophotometer, a JNM-ECA-400 NMR spectrometer. IR spectra were recorded on a Bio-RAD FTS-65A IR spectrophotometer. FAB-MS was recorded on a Micromass ZabSpec high-resolution mass spectrometer.

MT4 cells and human immunodeficiency virus type-1 (HIV-1_{IIIB}) virus were from the Center of AIDS, Beijing Institute of Microbiology and Epidemiology. Plasma from Kunming mice and Sprague−Dawley rats was prepared in our lab. Plasma from beagle dogs, monkey, and healthy humans was donated by Prof. G. Dou of Beijing Institute of Transfusion Medicine.

Kunming mice from the Laboratory Animal Center of Beijing Institute of Radiation Medicine (BIRM) were used. Principles in good laboratory animal care were followed, and animal experimentation was in compliance with the Guidelines for the Care and Use of Laboratory Animals in BIRM. Mice were sacrificed by euthanasia to remove tissues. Mouse tissue homogenates used in the experiments of chemical stability and tissue distribution were prepared in tissue/water (1:1, w/w).

Synthesis of the Prodrug. The synthesis procedure of ZPDD was divided into four steps (see Figure 1). Simply, deoxycholic acid was transformed to dehydrodeoxycholic acid followed by conjugation with ddI. The intermediate was reduced to deoxycholate that was then phosphorylated with phosphorus oxychloride. Finally, AZT was conjugated to obtain ZPDD. The details are described as follows.

Deoxycholic acid (20 mmol) was dissolved in acetone (100 mL) followed by incubation in 4 °C bath and agitation for 10 min. A Jones reagent (20 mmol, 10 mL) was added. The reaction proceeded for 2 h. Most of solvents were removed under vacuum. The residue liquid was transferred to a separatory funnel and diluted with dichloromethane (DCM, 30 mL). The organic solution was washed with the saturated $NaHCO_3$ solution repeated until the color disappeared. The DCM phase was separated and dried with anhydrous Na_2SO_4. The solvent was removed to obtain the white solid of dehydrodeoxycholic acid ($C_{24}H_{36}O_4$) with about 80% yield.

Dehydrodeoxycholic acid (60 mmol), ddI (20 mmol), *N*,*N*′-dimethyl aminopyridine (DMAP, 4 mmol), and *N*,*N*′-dicyclohexyl carbodiimide (DCC, 24 mmol) were together dissolved in *N*,*N*′-dimethylformamide (DMF, 100 mL) followed incubation at 45 °C and agitation for 2 days. Most of solvents were removed under vacuum. The residue liquid was transferred to a separatory funnel and diluted with DCM (50 mL). The organic solution was washed with the citric acid solution (0.5 mmol/L), the saturated $NaHCO_3$ solution, and water in turn. The DCM phase was separated and dried with anhydrous Na_2SO_4. The solvent was removed to obtain a slightly yellow solid. The solid was then purified on a silica chromatographic column with eluent of DCM/ethanol of the volume ratios from 50:1 to 30:1 to obtain the white powder of didanosine dehydrodeoxycholate ($C_{34}H_{46}N_4O_6$) with about 70% yield.

Didanosine dehydrodeoxycholate (1 mmol) and sodium borohydride (1 mmol) were dissolved in ethanol (20 mL) followed by agitation at room temperature for 2 h. Most of solvents were removed under vacuum. The residue liquid was mixed with water (20 mL) and then extracted with ethyl acetate (20 mL). The ethyl acetate phase was separated and dried with anhydrous Na_2SO_4. The solvent was removed to obtain the white solid of didanosine deoxycholate ($C_{34}H_{50}N_4O_6$) with more than 90% yield.

Didanosine deoxycholate (1 mmol) and $POCl_3$ (2.2 mL) were dissolved in DCM (20 mL) and agitated in ice bath for 2 h. Zidovudine (1 mmol) was dissolved in DCM (20 mL) and then added with triethylamine (0.4 mL). The solution was dropped into the didanosine deoxycholate solution and agitated at room temperature overnight. The reaction solution was transferred to a separatory funnel and washed with the citric acid solution (0.5 mM), the saturated $NaHCO_3$ solution and water in turn. The organic phase was separated, dried with anhydrous Na_2SO_4. The solvent was removed to obtain a semisolid. The solid was purified on a silica chromatographic column with eluent of DCM/ethanol of the volume ratios from 30:1 to 15:1 to obtain the white powder of ZPDD ($C_{44}H_{62}N_9O_{12}P$) with 45% yield. TLC: chloroform/methanol (90:10, v/v), R_f = 0.7; UV (MeOH): λ_{max} = 266 nm; IR ν_{max}: 3409, 3194, 3065, 2930, 2818, 2106, 1690, 1551, 1466, 1371, 1319, 1269, 1181, 1036, 918, and 557 cm^{-1}; δ_H (400 MHz, $CDCl_3$): 0.6−2.2 (m, 33H), 2.2−2.5 (m, 9H), 3.57 (q, 1H, *J* = 3.4 Hz, OPO−CH, deoxylcholyl), 3.76 (q, 1H, *J* = 2.5 Hz, $CH_2CH(OH)C$, deoxylcholyl), 3.90, 4.23 (m, 4H, OPO-H, OCOCH), 3.93 (s, 1H, OH), 4.12 (q, 1H, *J* = 7.3 Hz, O−$CH$$CH_2$−OPO), 6.20 (t, 1H, *J* = 6.4 Hz, CH-thymidine), 6.25 (t, 1H, *J* = 6.5 Hz, CH-inosine), 7.29 (s, 1H), 7.45 (s, 1H), 7.54 (s, 1H), 9.39 (s, 1H), 9.41 (s, 1H); δ_C (100 MHz, $CDCl_3$): 12.6−32.6 (C-deoxycholic acid), 12.8 (CH_3), 38.0, 38.3 ($HCCH_2CH_2CH$), 60.8 (CHCH), 66.6 (N_3CC), 67.5 (2C, CCO), 83.6, 83.2 (3C, OCC), 104.0 (C, CCCO), 104.7 ($NCCCH_3$), 110.9 (NCCN), 135.4 (2C, NCN), 150.2 (2CO), 163.8 (CO); FAB-MS (+): 941.60, $(M + H)^+$ (17).

Solubility Measurement. A certain amount of ZPDD was mixed with solvents to obtain the suspensions that were agitated at 25 °C for 48 h to sufficiently dissolve. The saturated solutions were filtrated through the 0.45 μm membranes, and ZPDD in the filtrates was determined using high-performance liquid chromatography (HPLC).

Langmuir Monolayers at the Air−Water Interface. Surface pressure−area (π−A) isotherms were obtained using a KSV minitrough II film balance (KSV Instrument, Finland) equipped with the dual barriers and a Pt Wilhelmy plate sensing device. The area of the Teflon trough is 24 300 mm^2. The subphases were purified water, amine acetate buffered solution (pH 4.0, 20 mM), and Tris-HCl buffered solution (pH 9.0, 20 mM), respectively, and the temperature of subphases were controlled to 35 °C with the circulation water bath. ZPDD solution in chloroform (25 μL) was deposited onto the subphase with a Hamilton microsyringe precisely. Compression was initiated after a delay of 15 min to allow evaporation of the spreading solvent. The compression rate was 10 mm/min. π−A isotherms were recorded with a computer.

Preparation of the Self-Assemblies. The preparation of ZPDD self-assemblies was similar to the other self-assemblies of nucleoside lipid derivatives.[33,34] An injection method was used to prepare ZPDD self-assemblies. The ZPDD solution (5 mg/mL) in tetrahydrofuran (THF) was slowly injected into water using a 100 μL microsyringe under vortex agitation to get a homogeneous and slightly blue scattering transparent suspension of about 1 mg ZPDD/mL. After removing solvents and partial water by heat under vacuum, a stable concentrated suspension of ZPDD self-assemblies was obtained with the high concentration of ∼10 mg ZPDD/mL.

Characterization of the Self-Assemblies. The self-assemblies were observed using a Philips CM120 80 kV transmission electron microscope (TEM). Five microliters of the suspensions were dropped onto the carbon-coated copper nets and maintained for one minute. The redundant liquid was removed by filter paper from the edge of nets. A solution containing 2% sodium phosphotungstate (pH 6.5) was also dropped onto the above nets and processed as the above. The resulted negative-stained samples were air-dried at room temperature and moved to the TEM for observation as soon as possible.

The dynamic lighting scattering method was used to measure the particle size and size distribution of the assemblies on Zetasizer Nano ZS (Malvern, UK). The suspension was diluted with water until to about 0.1−0.6 mg/mL ZPDD, and then measured at 25 °C. The zeta potential of self-assemblies was also measured with the above instrument and the same process.

HPLC Measurement. HPLC experiments were performed on a Hitachi L-2130 HPLC system (Japan), consisting of L-2130 pump, L-2400 UV detector, and Hitachi D-2000 chromatographic workstation software. The Diamonsil C18-ODS columns (5 μm, 250 mm × 4.6 mm) and the EasyGuard C18-ODS guard columns (5 μm, 8 mm × 4 mm) were purchased from Dikma Co., Ltd. (China). A manual injection valve and a 20 μL loop (7725i, Rheodyne, USA) were used. The HPLC column temperature was kept at 30 °C with a HT-230A heater and cooler (Tianjin Hengao Technology Development Co., Ltd.). UV wavelengths were 266 nm. ZPDD and the possible degradation products (mainly AZT and ddI) in suspensions or in biological samples were simultaneously determined on HPLC with the

gradient mobile phase of the mixture of methanol and water. The mobile phase condition included: the volume ratios of methanol in the mixture ranging from 20% to 95% within 0 to 15 min, and the flow rate was 1.0 mL/min. The retention times (t_R) of ddI, AZT, and ZPDD were about 6.4, 9.5, and 13.4 min, respectively.

Stability Investigation of the Self-Assemblies. ZPDD self-assemblies belong to the nanoparticulate systems so that the physical stability should be considered. ZPDD is a prodrug. It is necessary for ZPDD to degrade to the parent drugs or active intermediates to perform treatment. Therefore, the chemical stability should be explored.

Heat could affect the physical stability of ZPDD self-assemblies. The self-assembly suspensions were sealed in ampules and processed with autoclave (121 °C, 15 pounds, 30 min) or boiling at 100 °C for 30 min. The sizes of ZPDD self-assemblies were measured after being cooled. Gravity could induce aggregation of the assemblies. The suspensions were centrifuged from 2000 to 10000 rpm for 5 min and resuspended for size measurement. The effect of long-term storage was also investigated. The suspensions of ZPDD self-assemblies were diluted with the buffered solutions of different pH values (pH 7.4, 5.5, 5.0, 4.0, and 3.0) and maintained for several hours. The sizes and zeta potentials were measured.

The degradation of ZPDD in buffered solutions, plasma, and tissue homogenates was investigated. The suspensions were diluted with the 3-fold volume of buffered solutions, including 0.01 M hydrochloride acid solution (pH 2.0) and 20 mM phosphate buffers (pH 5.0 and 7.4), and incubated at 37 °C. At predetermined time intervals, one aliquot of 10 μL was pipetted out and 10-fold diluted with methanol. The samples of plasma and tissue homogenates needed centrifugation at 5000 g for 10 min after methanol dilution. The dilutions or supernatants were determined with HPLC.

Cell Experiments. The anti-HIV effect of ZPDD self-assemblies was performed with reference to our previous research.[31,34] The HIV-1 infected MT4 cells were used as a model. The cultural medium was the RPMI-1640 (Sigma) solution supplemented with 10% calf serum and 1×10^5 units of penicillin and streptomycin. The suspension of self-assemblies and AZT aqueous solution were sterilized by the film filtration with the 0.22 μm filters. The medicines were 10-fold gradient-diluted with the cultural medium. The concentration of ZPDD in cell cultures was from 10 μM to 0.1 nM, in six levels with a 10-fold decreasing gradient and in triplicates every level. AZT aqueous solutions were as the controls with the same molar concentrations. After 72 h of incubation at 37 °C, the cytopathic effect (CPE) assay was performed with a light microscope, and the 50% effective concentration (EC_{50}) was deduced.

The toxicity of ZPDD self-assemblies was determined using the MTT test by measuring mitochondrial dehydrogenase activity on the above MT4 cell model. ZPDD was gradient-diluted by the cultural medium to 590.5, 118.1, 11.81, and 1.181 μM, respectively. The diluted medicines were added to the cells followed by incubation for 72 h. Every level was tested in triplicate. After 72 h, the MTT solution (5 mg/mL, 20 μL, Amresco) was added to each well. Four hours later, the cultural media were removed. The formed formazan crystals were dissolved in 150 μL dimethyl sulfoxide per well. The absorbance of converted dye was measured at 490 nm using a microplate reader (Multiskan MK3, Thermo Scientific). The cell viability was equal to experimental absorbance/control absorbance × 100%. The half toxic concentration (TC_{50}) was calculated by the ICp software using the LOGIT method (free software supplied by Dr. Tang Tao). AZT solution was used as the control.

Pharmacokinetic Study. The in vivo fate of ZPDD were studied after administration of ZPDD self-assemblies to mice (body weight, 20−24 g) through three routes including iv, intraperitoneal (ip), and per oral (po). The suspensions were quantitatively determined by HPLC and sterilized with the 0.22 μm filters. For the iv or ip route, the drug was injected through tail vein or peritoneum with the dose of 100 mg ZPDD/kg mice. The blood samples were collected from the opposite tail veins, put into heparinized centrifuge tubes at the predetermined time points, and centrifuged to isolate plasma at 3000 rpm for 10 min. The drug in plasma was determined as the above stability experiment. In the tissue distribution experiment, the animals were ethically sacrificed at the predetermined time points, and the tissues were removed, cleared, weighed, and disrupted to homogenates followed by the same process as above. For the po route, the same dose of ZPDD was orally administered after po administration of 0.2 mL antiacid agent (NaH_2PO_4-citric acid, pH 5.5, 50 mM) to each mouse in advance.

The bioavailability for the ip or po route can be calculated according to the following equation.

$$F = \frac{AUC_{0-120min(po/ip)}/Dose_{(po/ip)}}{AUC_{0-120min(iv)}/Dose_{(iv)}} \times 100\% \quad (1)$$

where F is the bioavailability, and AUC is the area under the drug concentration−time curve. Because the dose is the same for all of the routes, the above equation can be abbreviated as the following equation.

$$F = \frac{AUC_{0-120min(po/ip)}}{AUC_{0-120min(iv)}} \times 100\% \quad (2)$$

Pharmacokinetic parameters are calculated with the 3p87 pharmacokinetic software supplied by Prof. H. Song of BIRM. Statistically significant differences for multiple groups were deduced using a one-way ANOVA with a Dunnett t test. All testing was done using SPSS 16.0 (SPSS Inc.).

RESULTS

Solubility of ZPDD. The solubility of ZPDD was different from traditional lipophilic compounds. The solubility of ZPDD in chloroform and THF was high (>125 mg/mL) but low in cyclohexane (3.6 mg/mL). The nucleobase-containing chemicals tend to form intermolecular hydrogen bonding between themselves in noncompetitive solvents (the solvents having poor hydrogen bonding donors and acceptors) such as chloroform and THF.[35] The hydrogen-bonding association of ZPDD in chloroform and THF may lead to the high solubility. ZPDD was soluble in octanol (15.8 mg/mL), slightly soluble in methanol (2.64 mg/mL), and insoluble in water.

Monolayer Behavior of ZPDD at the Air−Water Interface. The $\pi-A$ isotherms of Langmuir monolayers can provide the conformation information of amphiphilic molecules at the interface.[36] ZPDD showed monolayer behavior different from normal amphiphiles at the air−water interface. The $\pi-A$ isotherms of ZPDD monolayers had a much larger onset molecular area than that of another amphiphilic prodrug, cholesteryl-phosphoryl zidovudine (CPZ), containing the same polar head as ZPDD. The difference should result from the two polar heads of the bolaamphiphilic ZPDD molecules that

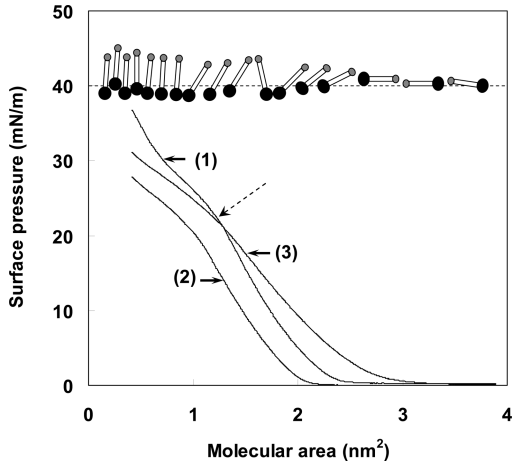

Figure 2. $\pi-A$ isotherms of ZPDD monolayers at the different interfaces and the illustration of monolayer behavior. The interfaces are air−water (Curve 1), air−amine acetate buffered solution (pH 4.0, 20 mM) (Curve 2), and Tris-HCl buffered solution (pH 9.0, 20 mM) (Curve 3), respectively. The larger filled circles represent the phosphoryl zidovudine groups, the smaller circles are the ddI groups, and the long sticks are the deoxycholyl groups. The arrow point indicates the inflections that all of the curves have.

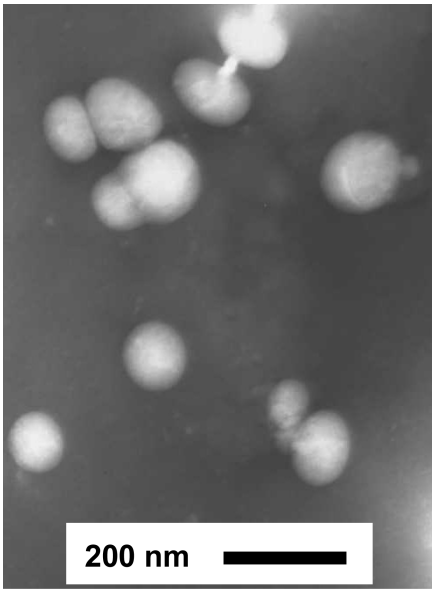

Figure 3. TEM image of ZPDD self-assemblies.

could lie on the interface with two heads contacting the subphase (Figure 2). In contrast, the amphiphilic CPZ molecules could only stand or tilt at the interface at the initial compression field. The lying conformation should lead to the large onset molecular area of ZPDD monolayer. In the whole compressing process, the phosphoryl zidovudine groups were prone to insert into the subphase due to its larger volume and higher hydrophilicity than the other polar head ddI group. When compression continued, the molecules could undergo a tilt-to-stand process, and the highly compressed molecules could partially overlap. The following slowly lifting curves of ZPDD monolayers could indicate the molecules inserting and overlapping the adjacent ones. The isotherms of ZPDD monolayers had the inflections at 20 mN/m,

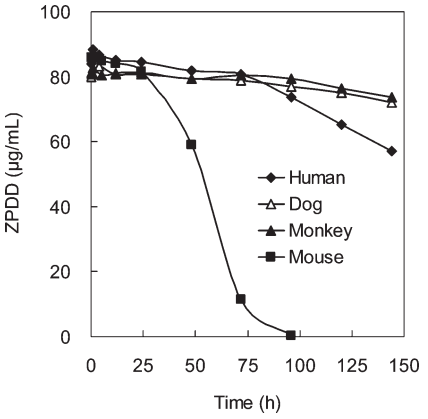

Figure 4. Degradation of ZPDD in the different plasma. The data are the means of two replicates.

suggesting that the molecules could basically stand at this time. After the inflection, the surface pressure increased along with the further compression, similar to the behavior of CPZ monolayer. In the end of compression, the heads could be squeezed out over the interface. Unfortunately, the compression did not proceed after the molecular area got to about 0.5 nm^2 because of the limit of trough area. Interestingly, the $\pi-A$ isotherms of ZPDD monolayers were sensitive to the subphase pH values. Comparing the isotherms with three types of subphases including pH 9.0 buffers, water, and pH 6.0 buffers, the first isotherm showed the earliest lift-off point and the largest onset molecular area than the others (Figure 2).

Characteristics of the Self-Assemblies. ZPDD self-assemblies were the spherical vesicles according to the TEM image (Figure 3). The self-assembly suspension was homogeneous and nearly transparent. ZPDD self-assemblies had a small mean size of 174 nm and a narrow size distribution. The high zeta potential (−31.3 mV) of assemblies was related to phosphoryl dissociation and improved repulsion between particles. A concentrated suspension (∼10 mg/mL ZPDD) was obtained without any precipitant.

Interestingly, the sizes and zeta potentials of assemblies depended on pH. The mean sizes were 143, 144, 270, 288, and 1107 nm at pH 7.4, 5.5, 5.0, 4.0, and 3.0, respectively. The zeta potentials were −32.5, −27.8, −19.2, −8.4, and −2.3 mV in the above turn, respectively. The monolayer experiment had shown that acid inhibited phosphoryl association. Therefore, the low pH environment resulted in the low surface charge of assemblies, and then the little charged assemblies was prone to aggregation. The phenomena demonstrated that the phosphoryl zidovudine groups could dominate in the outer surface of self-assembled vesicles, while the ddI groups could dominate in the inner surface.

Stability of ZPDD Self-Assemblies. The heat process did not change the size of ZPDD self-assemblies when autoclave or boiling was applied. The size of assemblies was only from 174 to 178 nm after heating. However, it was found that the degradation of ZPDD happened in the heated samples. Therefore, heat sterilization could not be accepted. The film filtration was used for sterilization. To accelerate gravity effect on the stability of ZPDD self-assemblies, the high centrifugation was applied. It was found that ZPDD self-assemblies kept stable under high centrifuge. Furthermore, the storage at room temperature for more than one month did not affect the appearance and size of ZPDD self-assemblies.

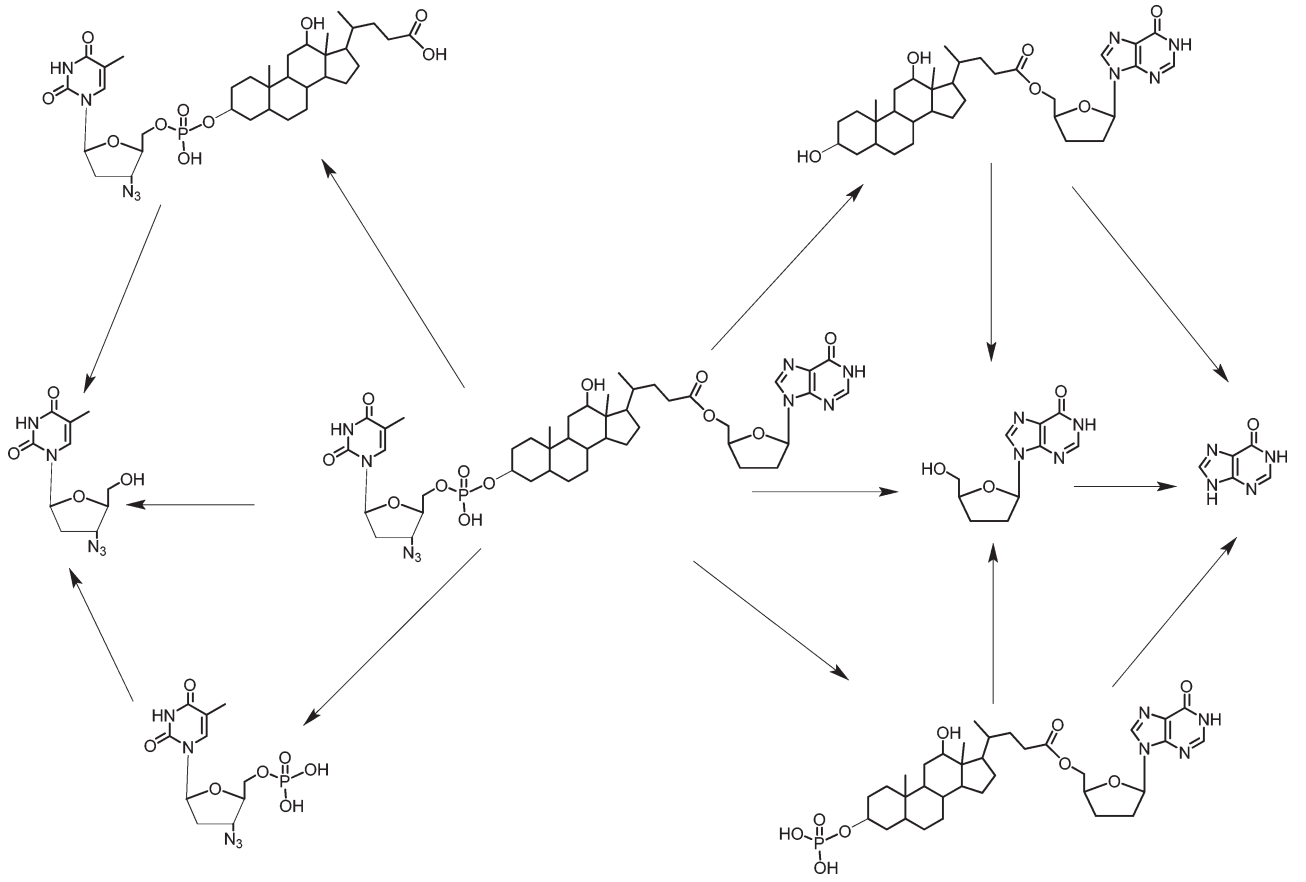

Figure 5. Possible metabolic routes of ZPDD.

ZPDD needs to degrade to the active parent drugs or intermediates. It was found that ZPDD degradation highly depended on pH. pH 2.0, 5.5, and 7.4 represent the environment in the stomach, intestine, and blood, respectively. ZPDD degraded in acidic solutions but kept stable in neutral media. All ZPDD was nearly degraded within 0.5 h at pH 2.0. The degradation half-life ($t_{1/2}$) of ZPDD was 61.3 h at pH 5.5 and more than 1000 h at pH 7.4.

ZPDD degradation was different in the plasma of humans, dog, monkey, and mouse (Figure 4), wherein the mouse plasma had the strongest ability with the degradation $t_{1/2}$ of 9 h. The species differences of enzyme activity is the major reason.[37] Furthermore, the $t_{1/2}$ in mouse liver homogenates was only 3 h. The rapid degradation of ZPDD might produce the parent drugs or active intermediates such as phosphoryl zidovudine. The possible degradation mechanism of ZPDD is shown in Figure 5.

In Vitro Antiviral Activity of the Self-Assemblies. Anti-HIV action and the toxicity of ZPDD self-assemblies were explored on the HIV-1 infected MT4 cells with AZT solution as a control. ZPDD had the high anti-HIV activity with the half effective concentration (EC_{50}) of 5 nM, equal to the EC_{50} of AZT. The half toxic concentration (TC_{50}) of ZPDD was 42.22 μM, so that the selection index (SI) of ZPDD self-assemblies was 8444. In contrast, the TC_{50} of AZT was 283.17 μM.

In Vivo Fate of ZPDD Self-Assemblies. ZPDD self-assemblies showed the different pharmacokinetic profiles and tissue distribution after administration to mice through the iv, ip, and po routes (Figure 6). Little ZPDD appeared in the heart and brain after administration, but a lot occurred in the spleen, lymph node, thymus, liver, and lung (Figure 6b), and a great number of phagocytes were present in the latter tissues.[38] The phagocyte targeting effect was related to the nanoscale nature of assemblies. Interestingly, the molar concentration of AZT was much higher than that of ZPDD in the targeted tissues (Figure 6c). The rapid degradation of ZPDD in the targeted tissues should be responsible for this. The in situ high concentration of AZT would favor AIDS treatment. However, the concentration of ddI was comparable with that of ZPDD in the targeted tissues (Figure 6d). Maybe ddI was produced more slowly than AZT, and the metabolites of ddI were produced.

The detailed pharmacokinetic parameters are shown in Table 1. The bioavailability of ZPDD was 90.5% and 30.8% after the ip and po administration compared with the iv route. The high ip bioavailability may be related to the lipophilic property of ZPDD.[39] The low oral bioavailability may be related to the instable properties in stomach, the enzyme damage, and the insufficient absorption of ZPDD self-assemblies, although one antiacid agent was administered in advance. Interestingly, in the case of the ip route, the elimination rate constant (k_e) was smaller than the other routes, and a longer elimination $t_{1/2}$ was shown. The absorption of ZPDD could be slow from peritoneum, and there was a continual absorption in the field of elimination based on the pharmacokinetic profile (Figure 6a). For the po route, the apparent distribution volume (V_d) was much more than the other routes. This might be related to the lymph absorption of ZPDD from small intestine due to the lipophilic and nanoparticulate properties.[40,41]

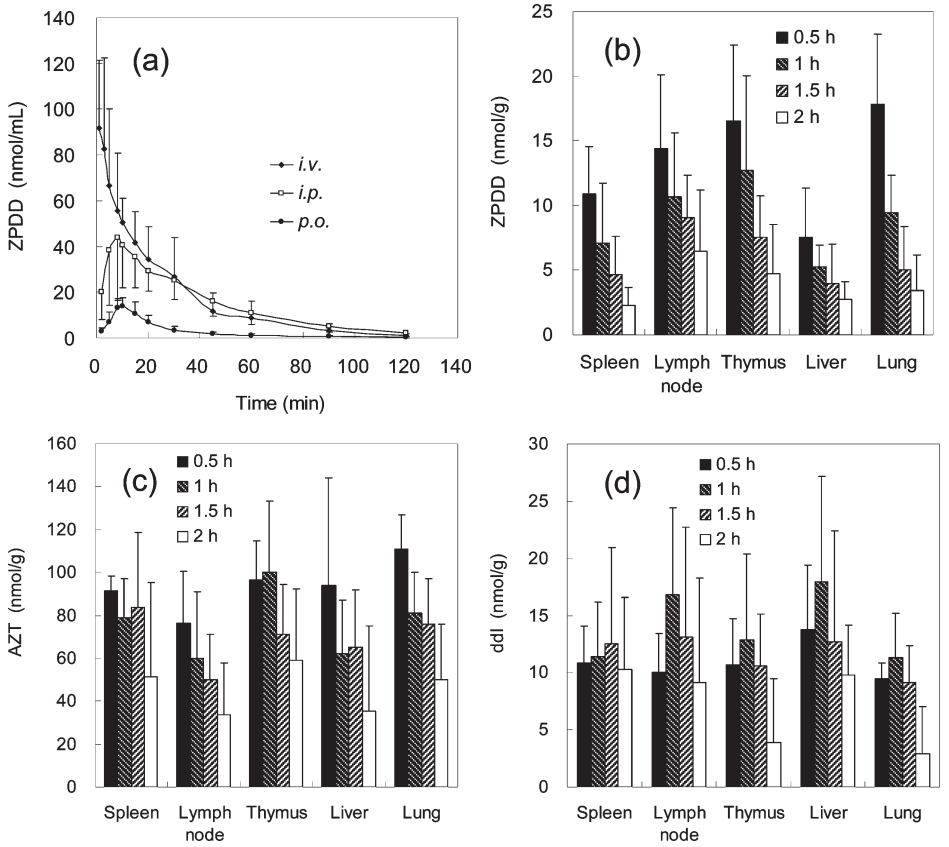

Figure 6. Profiles of ZPDD concentration in circulation (a) after administration of ZPDD self-assemblies to mice through three routes, and the tissue distribution of ZPDD (b), AZT (c), and ddI (d) after the iv administration of ZPDD self-assemblies to mice. $N = 5$.

Table 1. Pharmacokinetic Parameters of ZPDD after Administration of ZPDD Self-Assemblies to Mice

parameters	values[a]		
	iv	ip	po
k_e/min^{-1}	0.047 ± 0.023	0.026 ± 0.006	0.053 ± 0.018
$t_{1/2}$/min	17.8 ± 6.5	28.1 ± 7.8	15.7 ± 7.6
V_d/mL	1.42 ± 0.28	2.44 ± 1.30	7.96 ± 7.40
Cl/mL·min^{-1}	0.065 ± 0.026	0.063 ± 0.040	0.30[b] ± 0.15
C_{max}/μg·mL^{-1}	—	41.4 ± 26.0	10.0 ± 4.8
t_{max}/min	—	8.24 ± 2.80	9.77 ± 4.50
$AUC_{0-120\ min}$/μg·mL^{-1}·min	1868 ± 829	1690 ± 438	575 ± 630

[a] The values are the means ± SD, $n = 5$. k_e, the elimination rate constant. $t_{1/2}$, the elimination half-life time. V_d, the apparent distribution volume. Cl, the clearance rate. C_{max}, the maximum drug concentration. t_{max}, the time reaching C_{max}. $AUC_{0-120\ min}$, the area under the drug concentration–time curve between 0 to 120 min. [b] $P < 0.01$, po vs iv or ip

DISCUSSION

The aim of this study is to obtain a stable self-assembled system of bolaamphiphilic prodrugs to target to pathological tissues and release the active drugs with an appropriate rate. Therefore, the self-assembling property, stability, activity, body deposition, and metabolism of ZPDD are focused on. The design of ZPDD is also based on the above aim and the related requests.

The amphiphilic ZPDD had the special solubility in different solvents, suggesting that ZPDD is lipophilic and tends to form hydrogen bonds. The phenomenon is similar to the other lipid derivatives of AZT and ddI.[33] The highly concentrated solution of ZPDD in THF is also a good option as the injection solution to prepare self-assemblies.

Langmuir monolayer experiment is a common method to characterize amphiphiles. ZPDD showed the unique Langmuir monolayer behavior. ZPDD molecules could lie on the water surface with two heads contacting water at the beginning of compression. The special conformation is the typical behavior of bolaamphiphiles at the interface.[31,42] Significantly, the phosphoryl groups of ZPDD tended to dissociate hydrogen ions into the subphases, and the dissociation should be inhibited by acid and improved by alkaline. The stronger ZPDD dissociation was, the higher the head charges, and then the stronger the intermolecular repulsion. Therefore, ZPDD had a earlier lift-off point and larger molecular area in the higher pH subphase than the lower pH subphase. The pH sensitivity also demonstrated that the phosphoryl zidovudine groups should dominate at the interface.

The driving force of ZPDD self-assembly should be hydrophobic interaction between the deoxycholyl groups, like other nucleoside lipid derivatives.[33] The interaction could lead to the formation of soft ZPDD monolayers further bending to the closed vesicles. Which surface of the monolayer one of two heads of ZPDD dominated is not known now. There is no suitable method to give sufficient proofs to indicate which head dominates in the inner or outer surface of vesicles. However, according to the volume of heads, most of the larger phosphoryl zidovudine

groups might distribute in the outer surface due to the larger area, while most of the smaller ddI groups might exist in the inner surface. The high negative zeta potential of ZPDD self-assemblies indicated the release of hydrogen ions of phosphoryl groups to the surroundings, which was evidence of the phosphoryl zidovudine groups existing in the outer surface. In addition, the pH sensitivity of self-assemblies also indicated that phosphoryl groups could dominate the outer surface of self-assemblies.

The degradation of ZPDD was highly related to its molecular structure. ZPDD had three ester bonds, resulting in rapid degradation in the high or low pH media, as in the other reports.[31,32,34] Therefore, antiacid agents should be orally administered before po administration of the assemblies. Esterases were widely present in body so that it was not surprising that ZPDD was rapidly degraded in plasma or tissues. The rapid degradation was favorable because the inhibition of virus needed enough drugs. In our previous study, no antiviral activity was observed because the degradation of the lipid derivative of ddI was very slow.[43]

The high in vitro anti-HIV activity of ZPDD demonstrated that the self-assemblies could enter into cells and rapidly degrade to active drugs. The active drugs could include AZT, and the intermediate phosphoryl zidovudine that had been demonstrated as a potent anti-HIV intermediate.[44] However, the release of ddI could be slow because the bond between carboxyl and ddI might be destroyed with difficulty.[43] A little toxicity of ZPDD could be related to its amphiphilicity, involving the molecular insertion of cell membranes. Another amphiphilic nucleoside derivative also showed the similar effect.[32] However, the self-assemblies could be quickly optimized by plasma proteins in circulation after iv administration so that there was no opportunity to destroy the cell membranes such as erythrocytes before reaching targeted sites. Our previous research showed that another self-assembly does not lead to hemolysis in the whole blood of rabbits because of protein absorption in spite of the hemolysis of erythrocytes.[32]

ZPDD self-assemblies are mainly distributed in the macrophage-sufficient tissues. Macrophages constitute one of the most important viral reservoirs outside the bloodstream and are able to transport HIV into the central nervous system. Most of current anti-HIV drugs distribute in monocytes/macrophages not well so that eradication of HIV is very hard.[16,17] Therefore, ZPDD self-assemblies could be a good alternative method against latent HIV. ZPDD self-assemblies might be iv administered to eliminate the virus in macrophages after a long-term anti-HIV therapy with traditional HAART. The good bioavailability of ip administration indicates that ZPDD self-assemblies might be administered through intramuscular injection in the future clinical application. Generally, nanoparticles could be instable in the gastrointestinal tract. ZPDD could be absorbed in the molecular state, and the absorption efficacy was determined by its intrinsic property.

The asymmetric bolaamphiphilic prodrugs like ZPDD only contain two drug heads, so that the drug ratio is limited to 1:1. However, the 1:1 molar ratio may not be a good combination of drugs for some diseases. Furthermore, the current combination therapy is constructed based on free drugs, not bolaamphiphilic prodrugs, though some codrugs have been prepared. Therefore, the appropriate drugs for the preparation of bolaamphiphilic prodrugs should be explored in detail. We also look forward to find a novel prodrug technique combining the suitable drug ratios rather than 1:1.

In this study, a novel bolaamphiphilic prodrug-ZPDD was designed based on the SADDS theory and the need of anti-HIV therapy. Unlike AZT-P-ddI that was rapidly metabolized before reaching the target cells, the bolaamphiphilic ZPDD can simultaneously deliver two different drugs to the targeted cells, also the HIV reservoir, macrophages. This is a new progress of antiviral therapy and SADDS research. High stability, rapid release of at least one of the two parent drugs, and potentially good macrophage targeting effect of ZPDD self-assemblies demonstrate that the assemblies would become one promising anti-HIV nanomedicine. Combination therapy is widely applied in various diseases. However, the components of combination could not be sure to enter into the targeted cells simultaneously and maintain the suitable concentration. One bolaamphiphilic prodrug of double AZT moieties with the spacer of pentadecanedioyl was previously prepared in our lab. Its self-assembly and the in vivo behavior were explored.[31] The self-assemblies mainly distributed in the liver, spleen, and testis after iv administration to rabbits followed by rapid production of AZT. The merit of ZPDD self-assemblies is to combine two different types of antiviral agents into one molecule so that they could simultaneously enter the targeted cells. ZPDD represents a novel combination technique, involving prodrug, bolaamphiphilic molecules, nanotechnology, biology, and medicine.

■ ASSOCIATED CONTENT

Supporting Information. Table S1. Solubility of ZPDD; Figure S1. $\pi-A$ isotherm of cholesteryl-phosphoryl zidovudine (CPZ); Figure S2. Structures of CPZ and ZPDD; Figure S3. Illustration of ZPDD monolayer behavior at the air−water interface with the surface pressure increasing; Figure S4. Photograph of the suspension of ZPDD self-assemblies; Figure S5. The relationship between pH and zeta potentials of ZPDD self-assemblies; Figure S6. The relationship between pH and sizes of ZPDD self-assemblies; Table S2. Effect of centrifugation on the size of ZPDD self-assemblies. This material is available free of charge via the Internet at http://pubs.acs.org.

■ AUTHOR INFORMATION

Corresponding Author

*Beijing Institute of Radiation Medicine, Department of Pharmaceutical Sciences, 27 Taiping Road, Beijing 100850, China. Tel.: +86-10-8821-5159. Fax: +86-10-6821-4653. E-mail: jinyg@bmi.ac.cn (Y.J.).

■ ACKNOWLEDGMENT

This work was supported by the National Natural Science Foundation of China (No. 30672542) and the National Key Technologies R&D Program for New Drugs (No. 2009ZX-09301-002). The authors also acknowledge Prof. Dr. Minghua Liu of CAS for useful discussion.

■ REFERENCES

(1) Barreiro, P.; García-Benayas, T.; Rendón, A.; Rodríguez-Novoa, S.; Soriano, V. Combinations of nucleoside/nucleotide analogues for HIV therapy. *AIDS Rev.* **2004**, *6*, 234–243.

(2) Sosnik, A.; Chiappetta, D. A.; Carcaboso, Á. M. Drug delivery systems in HIV pharmacotherapy: What has been done and the challenges standing ahead. *J. Controlled Release* **2009**, *138*, 2–15.

(3) Falandry, C.; Canney, P. A.; Freyer, G.; Dirix, L. Y. Role of combination therapy with aromatase and cyclooxygenase-2 inhibitors in patients with metastatic breast cancer. *Ann. Oncol.* **2009**, *20*, 615–620.
(4) Sanz, G.; Fuster, V. Fixed-dose combination therapy and secondary cardiovascular prevention: rationale, selection of drugs and target population. *Nat. Clin. Pract. Cardiovasc. Med.* **2009**, *6*, 101–110.
(5) Cappellacci, L.; Franchetti, P.; Vita, P.; Petrelli, R.; Grifantini, M. Synthesis and antitumor activity of a heterodinucleotide of BVDU and gemcitabine. *Nucleosides, Nucleotides Nucleic Acids* **2008**, 460–468.
(6) Guenther, S.; Nair, V. Binding modes of two novel dinucleotide inhibitors of HIV-1 integrase. *Bioorg. Med. Chem. Lett.* **2002**, *12*, 2233–2236.
(7) Romeo, S.; Parapini, S.; Dell'Agli, M.; Vaiana, N.; Magrone, P.; Galli, G.; Sparatore, A.; Taramelli, D.; Bosisio, E. Atovaquone-statine "double-drugs" with high antiplasmodial activity. *ChemMedChem* **2008**, *3*, 418–420.
(8) Song, X. R.; Zheng, Y.; He, G.; Yang, L.; Luo, Y. F.; He, Z. Y.; Li, S. Z.; Li, J. M.; Yu, S.; Luo, X.; Hou, S. X.; Wei, Y. Q. Development of PLGA nanoparticles simultaneously loaded with vincristine and verapamil for treatment of hepatocellular carcinoma. *J. Pharm. Sci.* **2010**, *99*, 4874–4879.
(9) Tardi, P. G.; Gallagher, R. C.; Johnstone, S.; Harasym, N.; Webb, M.; Bally, M. B.; Mayer, L. D. Coencapsulation of irinotecan and floxuridine into low cholesterol-containing liposomes that coordinate drug release in vivo. *Biochim. Biophys. Acta* **2007**, *1768*, 678–687.
(10) Zhan, P.; Liu, X. Designed multiple ligands: an emerging anti-HIV drug discovery paradigm. *Curr. Pharm. Des.* **2009**, *15*, 1893–1917.
(11) Busso, M.; Mian, A. M.; Hahn, E. F.; Resnick, L. Nucleotide dimers suppress HIV expression in vitro. *AIDS Res. Hum. Retroviruses* **1988**, *4*, 449–455.
(12) Rossi, L.; Serafini, S.; Franchetti, P.; Cappellacci, L.; Fraternale, A.; Casabianca, A.; Brandi, G.; Pierigé, F.; Perno, C.-F.; Balestra, E.; Benatti, U.; Millo, E.; Grifantini, M.; Magnani, M. Targeting nucleotide dimers containing antiviral nucleosides. *Curr. Med. Chem. Anti-Infect. Agents* **2005**, *4*, 37–54.
(13) Zhou, X. J.; Squires, K.; Pan-Zhou, X. R.; Bernhard, S.; Agrofoglio, L.; Kirk, M.; Duchin, K. L.; Sommadossi, J. P. Phase I dose-escalation pharmacokinetics of AZT-P-ddI (IVX-E-59) in patients with human immunodeficiency virus. *J. Clin. Pharmacol.* **1997**, *37*, 201–213.
(14) Aquaro, S.; Caliò, R.; Balzarini, J.; Bellocchi, M. C.; Garaci, E.; Perno, C. F. Macrophages and HIV infection: therapeutical approaches toward this strategic virus reservoir. *Antiviral Res.* **2002**, *55*, 209–225.
(15) Gavegnano, C.; Schinazi, R. F. Antiretroviral therapy in macrophages: implication for HIV eradication. *Antiviral Chem. Chemother.* **2009**, *20*, 63–78.
(16) Gupta, U.; Jain, N. K. Non-polymeric nano-carriers in HIV/AIDS drug delivery and targeting. *Adv. Drug Delivery Rev.* **2010**, *62*, 478–490.
(17) Neves, J. d.; Amiji, M. M.; Bahia, M. F.; Sarmento, B. Nanotechnology-based systems for the treatment and prevention of HIV/AIDS. *Adv. Drug Delivery Rev.* **2010**, *62*, 458–477.
(18) Mamo, T.; Moseman, E. A.; Kolishetti, N.; Salvador-Morales, C.; Shi, J.; Kuritzkes, D. R.; Langer, R.; von Andrian, U.; Farokhzad, O. C. Emerging nanotechnology approaches for HIV/AIDS treatment and prevention. *Nanomedicine* **2010**, *5*, 269–285.
(19) Fuhrhop, J.-H.; Wang, T. Bolaamphiphiles. *Chem. Rev.* **2004**, *104*, 2901–2937.
(20) Li, S.; Zheng, F.; Zhang, X.; Wang, W. Stability and rupture of archaebacterial cell membrane: a model study. *J. Phys. Chem. B* **2009**, *113*, 1143–1152.
(21) Ambrosi, M.; Fratini, E.; Alfredsson, V.; Ninham, B. W.; Giorgi, R.; Nostro, P. L.; Baglioni, P. Nanotubes from a vitamin C-based bolaamphiphile. *J. Am. Chem. Soc.* **2006**, *128*, 7209–7214.
(22) Iwaura, R.; Yoshida, K.; Masuda, M.; Ohnishi-Kameyama, M.; Yoshida, M.; Shimizu, T. Oligonucleotide-templated self-assembly of nucleotide bolaamphiphiles: DNA-like nanofibers edged by a double-helical arrangement of A-T base pairs. *Angew. Chem., Int. Ed.* **2003**, *42*, 1009–1012.
(23) Iwaura, R.; Yoshida, K.; Masuda, M.; Yase, K.; Shimizu, T. Spontaneous fiber formation and hydrogelation of nucleotide bolaamphiphiles. *Chem. Mater.* **2002**, *14*, 3047–3053.
(24) Kim, J.-M.; Thompson, D. H. Tetraether bolaform amphiphiles as models of archaebacterial membrane lipids: synthesis, differential scanning calorimetry, and monolayer studies. *Langmuir* **1992**, *8*, 631–644.
(25) Weissig, V.; Torchilin, V. P. Cationic bolasomes with delocalized charge centers as mitochondria-specific DNA delivery systems. *Adv. Drug Delivery Rev.* **2001**, *49*, 127–149.
(26) Fabio, K.; Gaucheron, J.; Giorgio, C. D.; Vierling, P. Novel galactosylated polyamine bolaamphiphiles for gene delivery. *Bioconjugate Chem.* **2003**, *14*, 358–367.
(27) Muzzalupo, R.; Trombino, S.; Iemma, F.; Puoci, F.; Mesa, C. L.; Picci, N. Preparation and characterization of bolaform surfactant vesicles. *Colloids Surf., B* **2005**, *46*, 78–83.
(28) Bussmann, H.; Wester, C. W.; Thomas, A.; Novitsky, V.; Okezie, R.; Muzenda, T.; Gaolathe, T.; Ndwapi, N.; Mawoko, N.; Widenfelt, E.; Moyo, S.; Musonda, R.; Mine, M.; Makhema, J.; Moffat, H.; Essex, M.; Degruttola, V.; Marlink, R. G. Response to zidovudine/didanosine-containing combination antiretroviral therapy among HIV-1 subtype C-infected adults in Botswana: two-year outcomes from a randomized clinical trial. *J. Acquir. Immune Defic. Syndr.* **2009**, *51*, 37–46.
(29) Luzuriaga, K.; Bryson, Y.; Krogstad, P.; Robinson, J.; Stechenberg, B.; Lamson, M.; Cort, S.; Sullivan, J. L. Combination treatment with zidovudine, didanosine, and nevirapine in infants with human immunodeficiency virus type 1 infection. *N. Engl. J. Med.* **1997**, *8*, 1343–1349.
(30) Jin, Y.; Chen, S.; Xin, R.; Zhou, Y. Monolayers of the lipid derivatives of isoniazid at the air/water interface and the formation of self-assembled nanostructures in water. *Colloids Surf., B* **2008**, *64*, 229–235.
(31) Jin, Y.; Qi, N.; Tong, L.; Chen, D. Self-assembled drug delivery systems. Part 5: Self-assemblies of a bolaamphiphilic prodrug containing dual zidovudine. *Int. J. Pharm.* **2010**, *386*, 268–274.
(32) Jin, Y.; Tong, L.; Ai, P.; Li, M.; Hou, X. Self-assembled drug delivery systems. 1. Properties and in vitro/in vivo behavior of acyclovir self-assembled nanoparticles (SAN). *Int. J. Pharm.* **2006**, *309*, 199–207.
(33) Jin, Y.; Xin, R.; Ai, P.; Chen, D. Self-assembled drug delivery systems. 2. Cholesteryl derivatives of antiviral nucleoside analogues: synthesis, properties and the vesicle formation. *Int. J. Pharm.* **2008**, *350*, 330–337.
(34) Jin, Y.; Xing, L.; Tian, Y.; Li, M.; Gao, C.; Du, L.; Dong, J.; Chen, H. Self-assembled drug delivery systems. Part 4. In vitro/in vivo studies of the self-assemblies of cholesteryl-phosphonyl zidovudine. *Int. J. Pharm.* **2009**, *381* (1), 40–48.
(35) Lutz, J.-F.; Pfeifer, S.; Chanana, M.; Thunemann, A. F.; Bienert, R. H-bonding-directed self-assembly of synthetic copolymers containing nucleobases: organization and colloidal fusion in a noncompetitive solvent. *Langmuir* **2006**, *22*, 7411–7415.
(36) Jin, Y.; Chen, S.; Xin, R.; Zhou, Y. Monolayers of the lipid derivatives of isoniazid at the air/water interface and the formation of self-assembled nanostructures in water. *Colloids Surf., B* **2008**, *64* (2), 229–235.
(37) Minagawa, T.; Kohno, Y.; Suwa, T.; Tsuji, A. Species differences in hydrolysis of isocarbacyclin methyl ester (TEI-9090) by blood esterases. *Biochem. Pharmacol.* **1995**, *49*, 1361–1365.
(38) Dou, H.; Destache, C. J.; Morehead, J. R.; Mosley, R. L.; Boska, M. D.; Kingsley, J.; Gorantla, S. Development of a macrophage-based nanoparticle platform for antiretroviral drug delivery. *Blood* **2006**, *108*, 2827–2835.
(39) Di Stefano, A.; Carafa, M.; Sozio, P.; Pinnen, F.; Braghiroli, D.; Orlando, G.; Cannazza, G.; Ricciutelli, M.; Marianecci, C.; Santucci, E. Evaluation of rat striatal L-dopa and DA concentration after intraperitoneal administration of L-dopa prodrugs in liposomal formulations. *J. Controlled Release* **2004**, *99*, 293–300.
(40) Garzon-Aburbeh, A.; Poupaert, J. H.; Claesen, M.; Dumont, P. A lymphotropic prodrug of L-dopa: synthesis, pharmacological

properties, and pharmacokinetic behavior of 1,3-dihexadecanoyl-2-[(S)-2-arnino-3-(3, 4-dihydroxyphenyl)propanoyl]propane-l,2,3-triol. *J. Med. Chem.* **1986**, *29*, 687–691.

(41) Nishioka, Y.; Yoshino, H. Lymphatic targeting with nanoparticulate system. *Adv. Drug Delivery Rev.* **2001**, *47*, 55–64.

(42) Meister, A.; Weygand, M. J.; Brezesinski, G.; Kerth, A.; Drescher, S.; Dobner, B.; Blume, A. Evidence for a reverse U-shaped conformation of single-chain bolaamphiphiles at the air-water interface. *Langmuir* **2007**, *23*, 6063–6069.

(43) Jin, Y.; Ai, P.; Xin, R.; Tian, Y.; Dong, J.; Chen, D.; Wang, W. Self-assembled drug delivery systems. Part 3. In vitro/in vivo studies of the self-assembled nanoparticulates of cholesteryl acyl didanosine. *Int. J. Pharm.* **2009**, *368* (1−2), 207–214.

(44) Mavromoustakos, T.; Calogeropoulou, T.; Koufaki, M.; Kolocouris, A.; Daliani, I.; Demetzos, C.; Meng, Z.; Makriyannis, A.; Balzarini, J.; Clercq, E. D. Ether phospholipid-AZT conjugates possessing anti-HIV and antitumor cell activity. Synthesis, conformational analysis, and study of their thermal effects on membrane bilayers. *J. Med. Chem.* **2001**, *44*, 1702–1709.